



# A promising wound dressing based on alginate hydrogels containing vitamin D3 cross-linked by calcium carbonate/D-glucono- $\delta$ -lactone

Arian Ehterami<sup>1</sup> · Majid Salehi<sup>2,3</sup> · Saeed Farzamfar<sup>4</sup> · Hadi Samadian<sup>5</sup> · Ahmad Vaez<sup>6</sup> · Hamed Sahrapeyma<sup>7</sup> · Sadegh Ghorbani<sup>8,9</sup>

Received: 14 December 2019 / Revised: 28 February 2020 / Accepted: 12 March 2020 / Published online: 19 March 2020  
© Korean Society of Medical and Biological Engineering 2020

## Abstract

In the present study, we fabricated vitamin D<sub>3</sub>-loaded alginate hydrogel and assessed its wound healing capability in the animal model. The various concentrations of vitamin D<sub>3</sub> were added to the pre-dissolved sodium alginate in deionized water and cross-linked by calcium carbonate in combination with D-glucono- $\delta$ -lactone. The microstructure, swelling behavior, weight loss, hemo- and cytocompatibility of the fabricated hydrogels were evaluated. In the last stage, the therapeutic efficacy of the prepared hydrogels was evaluated in the full-thickness dermal wound model. The scanning electron microscopy images showed that the prepared hydrogel was highly porous with the porosity of  $89.2 \pm 12.5\%$  and contained the interconnected pores. Weight loss assessment showed that the prepared hydrogel is biodegradable with the weight loss percentage of about 89% in 14 days. The results showed that the prepared hydrogels were hemo- and cytocompatible. The animal study results implied that alginate hydrogel/3000 IU vitamin D<sub>3</sub> group exhibited the highest wound closure present which was statistically significant than the control group ( $p < 0.05$ ). Moreover, the histological examinations revealed that hydrogel containing 3000 IU vitamin D<sub>3</sub> had the best performance and induced the highest re-epithelialization and granular tissue formation. All in all, this study suggests that alginate hydrogels with 3000 IU vitamin D<sub>3</sub> can be exploited as a potential wound dressing in skin tissue engineering.

**Keywords** Tissue engineering · Alginate hydrogel · Vitamin D<sub>3</sub> · Skin · Wound healing

Arian Ehterami, Majid Salehi and Saeed Farzamfar are co-first authors and contributed equally to this work.

✉ Majid Salehi  
msalehi.te1392@gmail.com

✉ Hadi Samadian  
h30samadiyan@gmail.com

Arian Ehterami  
arian.ehterami@srbiau.ac.ir

Saeed Farzamfar  
saeed.tums1991@gmail.com

Ahmad Vaez  
ahmadvaez@yahoo.com

Hamed Sahrapeyma  
hamed.sahrapeyma@yahoo.com

Sadegh Ghorbani  
sadegh.ghorbani@modares.ac.ir

<sup>1</sup> Department of Mechanical Engineering, Science and Research Branch, Islamic Azad University, Tehran, Iran

<sup>2</sup> Department of Tissue Engineering, School of Medicine, Shahroud University of Medical Sciences, Shahroud, Iran

<sup>3</sup> Tissue Engineering and Stem Cells Research Center, Shahroud University of Medical Sciences, Shahroud, Iran

<sup>4</sup> Department of Tissue Engineering and Applied Cell Sciences, School of Advanced Technologies in Medicine, Tehran University of Medical Sciences, Tehran, Iran

<sup>5</sup> Nano Drug Delivery Research Center, Health Technology Institute, Kermanshah University of Medical Sciences, Kermanshah, Iran

<sup>6</sup> Department of Tissue Engineering and Applied Cell Sciences, School of Advanced Medical Sciences and Technologies, Shiraz University of Medical Sciences, Shiraz, Iran

<sup>7</sup> Department of Biomedical Engineering, Science and Research Branch, Islamic Azad University, Tehran, Iran

<sup>8</sup> Department of Anatomical Sciences, School of Medical Sciences, Tarbiat Modares University, Tehran, Iran

<sup>9</sup> Interdisciplinary Nanoscience Center (iNANO), Aarhus University, Aarhus, Denmark

## 1 Introduction

Skin as the first defense line of the body plays a vital protecting role against the various pathogens and dehydration. Furthermore, skin as the largest organ of the integumentary system has other important functions in fluid homeostasis, thermal/sensory detection, temperature regulation, sensation, and also the synthesis of vitamin D [1]. However, this organ is so vulnerable in which mechanical trauma, surgical procedures, burns, aging or reduced blood circulations can damage the layers of the skin [2]. Generally, skin is composed of three different layers including epidermis, dermis, and hypodermis which is able to be self-healed after injuries, but wounds necessitate immediate treatment using proper wound dressing to aid the regeneration and healing process [3]. A proper wound dressing should be able not only to maintain the moisture of the wound but also absorb the excess exudate in the wounded site. Moreover, it is beneficiary for a wound dressing to has the ability to be loaded with a specific wound healing enhancer such as proper and specific drugs, the natural substance, vitamins and so on.

Biocompatible dressings provide a suitable platform for cell adhesion and mimic the same extracellular matrix (ECM) as the tissue microenvironment. Different natural, synthetic and hybrid polymers have been used for fabricating the effective dressing to improve cell attachment and proliferation [4–7]. Hydrogels have an appropriate 3D microstructure which can provide structural totality to tissue construction and controlled drug delivery. Generally, hydrogels are fabricated from hydrophilic polymers cross-linked by either chemical interaction and covalent bonds or physical intermolecular and intramolecular attractions [8]. Hydrogels offer a great number of advantages for wound healing augmentation, for instance, they are suitable for topical drug delivery to the wounded skin, they are useful to maintain the moisture of the wound, and applicable for wound exudate [9–11]. Moreover, a hydrogel as the drug delivery vehicle can maintain a stable local concentration of therapeutic agent over the healing period [12]. A wide variety of materials have been applied for hydrogel preparation such as PLGA, PLLA, alginate, collagen, cellulose etc. [13]. Alginate is a polysaccharide extracting from brown seaweed and bacteria. It has gained a great deal of attention as the tissue engineering biomaterial due to its biocompatibility, non-immunogenicity, and biodegradability [14]. This polymer can be cross-linked by calcium chloride ( $\text{CaCl}_2$ ), calcium carbonate  $\text{CaCO}_3$  or calcium sulfate ( $\text{CaSO}_4$ ) to prepare a 3D structure suitable for drug delivery and tissue engineering applications [15]. Polymer-blended or drug-loaded alginate hydrogels have been widely used to enhance the healing efficiency of wound dressing [16–18].

There are various types of pharmaceutical ingredients loadable into the hydrogels to enhance the healing efficiency of a specific wound dressing [19–21]. Vitamin  $\text{D}_3$  (1, 25-Dihydroxyvitamin  $\text{D}_3$ ), is one of the most effective therapeutic agents which has fascinating impacts on skin wound healing process. There is evidence that vitamin  $\text{D}_3$  enhances the proliferation and differentiation of both fibroblasts and keratinocytes which are two primary cell types involved in the skin wound healing [22, 23]. Besides, it has been shown that vitamin  $\text{D}_3$  can promote vascular regeneration [24]. Accordingly, in the way to develop a proper wound dressing we combined the positive properties of alginate hydrogel with biological properties of vitamin  $\text{D}_3$  and evaluated its wound healing efficacy in the animal model.

## 2 Materials and methods

### 2.1 Materials

Sodium alginate, vitamin  $\text{D}_3$ , penicillin, streptomycin, and D-glucono- $\delta$ -lactone (GDL) were purchased from Sigma-Aldrich (St. Louis, USA). 3-(4, 5-dimethylthiazol-2-yl)-2, 5 diphenyl tetrazolium bromide (MTT), Dulbecco's modified Eagle's medium: nutrient mixture F-12 (DMEM/F12), and fetal bovine serum (FBS) were purchased from Gibco, BRL (Eggenstein, Germany).

### 2.2 Hydrogel fabrication

Sodium alginate was dissolved in deionized water to obtain the final concentration of 20 mg/mL (2 wt%). Next, based on the previous studies, two different concentrations of vitamin  $\text{D}_3$  were added to the alginate solution (3000, 30,000 unit Vit  $\text{D}_3$ : 10 ml alginate) and mixed on the stirrer at room temperature [25–27]. Calcium Carbonate ( $\text{CaCO}_3$ ) (144 mM) was mixed with GDL (added to initiate ionization of  $\text{CaCO}_3$ ) at molar ratio of 0.5 at neutral pH to cross-link alginate hydrogel [28]. The prepared sodium Alg/Vit  $\text{D}_3$  solutions were mixed and then vortexed with  $\text{CaCO}_3$  suspension for 1 min. Finally, a fresh aqueous GDL solution added to the suspension and mixed well for another 1 min to activate the gelation process.

### 2.3 Hydrogel characterization

#### 2.3.1 Morphological properties

Scanning Electron microscope (SEM AIS2100, Seron Technology, South Korea) was used to observe the morphology and the ultrastructure of alginate hydrogel and Alg/30,000 IU  $\text{D}_3$ . The samples were frozen for 6 h at  $-80^\circ\text{C}$  and then the frozen gels were lyophilized using a

freeze drier (Telstar, Terrassa, Spain) for 48 h at  $-54\text{ }^{\circ}\text{C}$ . The lyophilized samples were sputter coated with a thin layer of gold using a sputter coater (SC7620, Quorum Technologies, England) and finally the imaging was done at an accelerating voltage of 20 kV.

### 2.3.2 Swelling studies

The swelling behavior of Alg/Vit D<sub>3</sub> hydrogels was measured in the phosphate buffered saline (PBS) solution (pH=7.4), at ambient temperature. The prepared hydrogel was lyophilized by using a freeze drier until a constant weight of the gel. Then, the specific amount of hydrogel (4 ml) was immersed in 20 ml PBS and kept at the room temperature for 3 days to swell [29]. The swelling percentages of samples were measured every 60 min for the first 6 h and then every 2 h for the remaining hours. Subsequently, the samples were extracted from the solution and weighted quickly. The measurements were done and equilibrium mass swelling percentages were calculated based on Eq. (1).

$$\text{Equilibrium mass swelling} = \frac{m_1 - m_0}{m_0} \times 100 \quad (1)$$

where  $m_0$  and  $m_1$  are the dried mass weight and the mass swollen weight of the gel, respectively.

### 2.3.3 Weight loss analysis

The weight loss of the prepared hydrogels in PBS solution (pH=7.4) was used to measure the degradation rate of hydrogels. In this regard, the specific amount of the dried hydrogel disk was weighed and equal-size samples were immersed in a falcon tube containing PBS solution (pH=7.4) (15 ml) at  $37\text{ }^{\circ}\text{C}$  [30]. At the specific time points (7 and 14 days) triplicate specimens for each group were taken out from PBS solution, dried, and weighted. Equation (2) was used to calculate the degree of weight loss.

$$\text{Weight loss\%} = \frac{W_0 - W_1}{W_0} \times 100 \quad (2)$$

where  $W_0$  is the initial weight of hydrogels and  $W_1$  is the dry weight after removal from the water.

## 2.4 Blood compatibility

Human blood was used to evaluate the compatibility of the hydrogel. For this purpose, human blood was anticoagulated and diluted with normal saline. The samples were incubated with 0.2 ml of the diluted blood at  $37\text{ }^{\circ}\text{C}$  for 60 min. Then, the samples were centrifuged at 1500 rpm for 10 min and the created supernatant was transferred to a 96-well plate where the absorbance was measured at 545 nm by utilizing

the Anthos 2020 (Biochrom, Berlin, Germany) microplate reader. The positive control was 0.2 ml diluted blood in 10 ml deionized water while the negative control was 0.2 ml diluted blood in 10 ml normal saline. Eventually, hemolysis degree was calculated using Eq. (3):

$$\text{Hemolysis\%} = \frac{D_t - D_{nc}}{D_{pc} - D_{nc}} \times 100 \quad (3)$$

where  $D_t$  is the absorbance of the sample,  $D_{nc}$  indicates the absorbance values of the negative control,  $D_{pc}$  is the absorbance values of the positive control.

## 2.5 Cell viability studies

The MTT assay was used to quantitatively assess the cytotoxicity of the prepared hydrogels. Briefly, the mouse L929 murine fibroblastic cell line was cultured at the density of  $5 \times 10^3$  cells on the hydrogels in DMEM/F12 culture media supplemented with 10% (v/v) FBS, 100 unit/ml of penicillin and 100  $\mu\text{g/ml}$  of streptomycin in a humidified incubator at  $37\text{ }^{\circ}\text{C}$  with 5%  $\text{CO}_2$ . At each time point (1 and 3 days after cells seeding), the culture medium was removed from the 96-well plate and 0.2 ml of MTT (0.5 mg/ml) was added to each well, and the cells were incubated at  $37\text{ }^{\circ}\text{C}$  for 4 h in a dark place. Then, the solution was removed and 0.1 ml DMSO was added to each well to dissolve the formed formazan crystals [31, 32]. The absorption values of the samples were measured at a wavelength of 570 nm by means of a microplate reader Anthos 2020 (Biochrom, Berlin, Germany).

## 2.6 In vivo wound healing study

The wound healing ability of the prepared hydrogels was assessed in the full-thickness excisional wound model. Twenty-four healthy adult male Wistar rats (200–220 g) of 2 months of age were purchased from Pasteur Institute (Tehran, Iran). Animal experiments were approved by the ethics committee of the Kermanshah University of Medical Sciences (IR.KUMS.REC.1398.807) and were carried out in accordance with the university's guidelines. Intra-peritoneal injection of the mixture of Ketamine (Alfasan, Woerden, The Netherlands; 75 mg/1000 g body weight) and Xylazine (Alfasan, Woerden, The Netherlands; 7 mg/1000 g body weight) was used to induce the general anesthesia. Afterward, a  $1.50 \times 1.50\text{ cm}^2$  full-thickness wound was excised using a scalpel blade on the back skin of rats near the neck posterior surface. The animals were then randomly divided into four groups (6 rats in each group) and the wounds were treated with alginate hydrogel without vitamin D<sub>3</sub>, alginate hydrogel/3000 IU vitamin D<sub>3</sub>, alginate hydrogel/30,000 IU vitamin D<sub>3</sub>, and

sterile gauze as the negative control. The hydrogels were then mounted on the injury site using an elastic adhesive bandage.

The wound closure rate was recorded by a digital camera (Canon Inc., Tokyo, Japan) at the 7 and 14 days post-treatment and the wound area was measured by an image analyzing program (Digimizer, Ostend, Belgium). Finally, the wound closure was calculated via Eq. (4) [33]:

$$\text{Wound closure (\%)} = \left( 1 - \frac{\text{Open wound area}}{\text{Initial wound area}} \right) \times 100 \quad (4)$$

After 14 days of wounding, animals were sacrificed by injection of anesthetic drugs (150 mg ketamine and 20 mg Xylazine/kg body weight). The wound site was excised, and then the tissue was processed for histological evaluation. The treated wound specimens were immediately fixed with paraformaldehyde (4% in PBS, 0.01 M, and pH 7.4), sectioned, and stained with hematoxylin–eosin (H&E) and Masson's trichrome (MT) staining after processing and embedding in paraffin to evaluate the best stage of healing. The stained specimens were observed and interpreted by an independent pathologist under a light microscope (Olympus, Tokyo, Japan) with a digital camera (Olympus, Tokyo, Japan). The re-epithelialization, the thickness of the deposited collagen, and histomorphometry analysis were conducted to confirm the healing process.

## 2.7 Statistical analysis

The obtained data were statistically analyzed by the SPSS program, v.23 (IBM, Armonk, NY, USA) using one-way ANOVA test with Tukey's multiple comparison test ( $p < 0.05$ ). In all of the evaluations, the results were expressed as a mean  $\pm$  standard deviation and,  $p < 0.05$  was considered as statistically significant.

## 3 Results

### 3.1 Morphological studies

The morphology of the Alginate hydrogel and Alg/30,000 IU D3 hydrogel was observed by SEM (Fig. 1). Looking over the morphology of prepared hydrogel, it is found that the hydrogels have a highly porous structure with interconnected pores which were created through the phase separation during the lyophilization process. The porosity of alginate hydrogel was  $89.2 \pm 12.5\%$ . By adding Vit D to the prepared hydrogel, the percent of porosity increased to  $91.04 \pm 5.7\%$ . The differences between two samples are not significant. The Image J (National Institutes of Health, Bethesda, USA) and Origin Pro 2015 software (Origin Lab, Northampton, USA) was used to evaluate average diameters of the pores for both groups. For this purpose, a total of 20 random points per image were analyzed. The analytical results indicated that the pore size of prepared hydrogels was in the range of 75 to 135  $\mu\text{m}$ , which is favorable for cell attachment and migration [34].

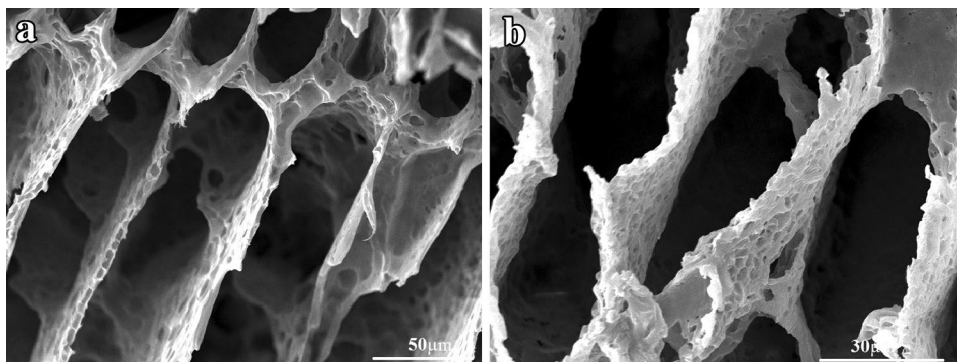
### 3.2 Swelling percentage of Alg/Vit D<sub>3</sub> hydrogels

Swelling indicated the liquid absorption by the hydrophilic polymer and it could be assessed by calculating the hydrogel mass. Figure 2a depicts the time course of the swelling. The results revealed that the mass swelling ratio of the alginate hydrogels were 124, 336 and 132% in the time of 60, 240 and 600 min, respectively. Additionally, the statistical findings from this experiment showed that the amount of swelling over time increases to 240 min, and then decreases.

### 3.3 Weight loss measurements

Figure 2b shows the weight loss percentages of the alginate gel in PBS. Biodegradation of hydrogels would depend on several factors including; the polymer density, the molecular weight of the polymer, the hydrophilicity behavior of

**Fig. 1** a Scanning electron microscopy of a Alginate hydrogel, b Alg/30,000 IU D3



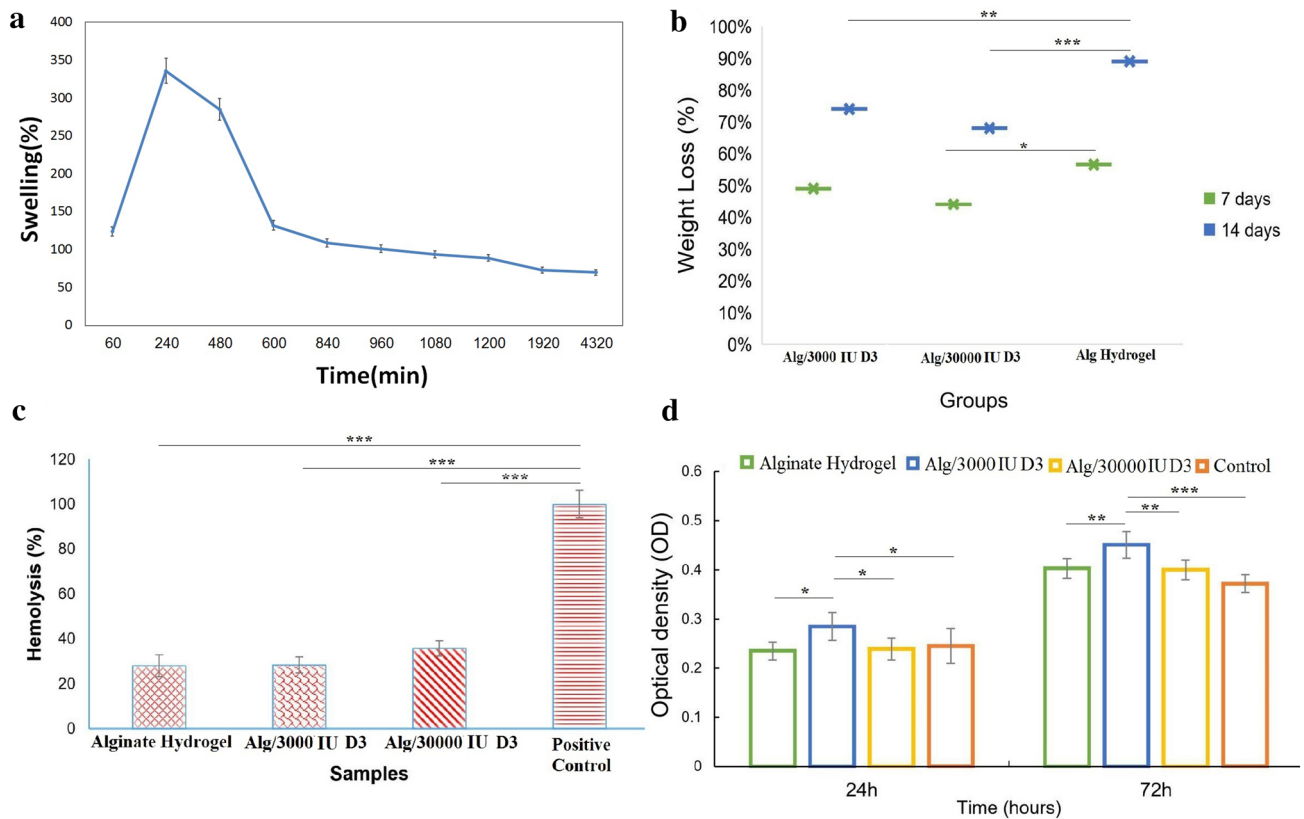


**Fig. 2** **a** Swelling percentages of the alginate hydrogel over time, **b** Weight loss percentage of the fabricated hydrogels at different time points (7 and 14 days), **c** Blood compatibility histogram of the experi-

mental samples, **d** MTT assay histogram after 24 and 72 h post cell seeding. Values represent the mean  $\pm$  SD,  $n=3$ , \* $p < .05$ , \*\* $p < .01$ , and \*\*\* $p < .001$ . SD: standard deviation

polymers, the position, and the number of linkage points susceptible to hydrolysis (e.g., ester bonds and so on) [35].

Degradation analysis showed that the degradation profile of prepared hydrogels was in the acceptable range of 45 to 89% during 14 days. The highest weight loss was observed in alginate hydrogel group. In other word, almost 89% of the initial weight of the alginate hydrogel has been lost after 2 weeks of storage in PBS. There was a significant difference in the percentage of the biodegradability between the alginate hydrogel and Alg/30000 IU D3 groups (Fig. 2b).

### 3.4 Blood compatibility or hemolysis assay

The interaction of the biomaterials with the blood component is a critical step and determine the fate of the biomaterials and the success of the treatment. Hemolysis is the rupturing of the erythrocytes (red blood cells) membrane and release of the hemoglobin into plasma. This phenomenon is directly related to the blood compatibility of materials. The hemocompatibility results (Fig. 2c) showed that the hemolysis of the prepared hydrogels was significantly lower than the positive control group.

### 3.5 Cell toxicity studies

MTT assay was carried out to further evaluate L929 the biocompatibility of the prepared hydrogels. The cell viability was measured hydrogels at 24 and 72 h after cell seeding and the results are shown in Fig. 3d.

As is shown in Fig. 3d, the prepared alginate hydrogels are not only biocompatible but also could stimulate the cells growth and proliferation in an obvious dose-dependent manner at 24 and 72 h. The MTT results showed that the proliferation rate of L929 cells on Alg/3000 IU D3 group was higher than other groups at 24 h after cell seeding (Fig. 3d). The cell viability of this group was statistically higher than the positive control (Tissue Culture Plate) and alginate hydrogel.

Moreover, the cells proliferation on the alginate hydrogel containing vitamin D<sub>3</sub> 3000 IU was significantly higher than the other groups at 72 h post cell seeding. Generally, the findings of cell viability studies revealed that the incorporation of vitamin D<sub>3</sub> in alginate hydrogels made these engineered hydrogels more suitable for cell proliferation due to its cytocompatible nature.

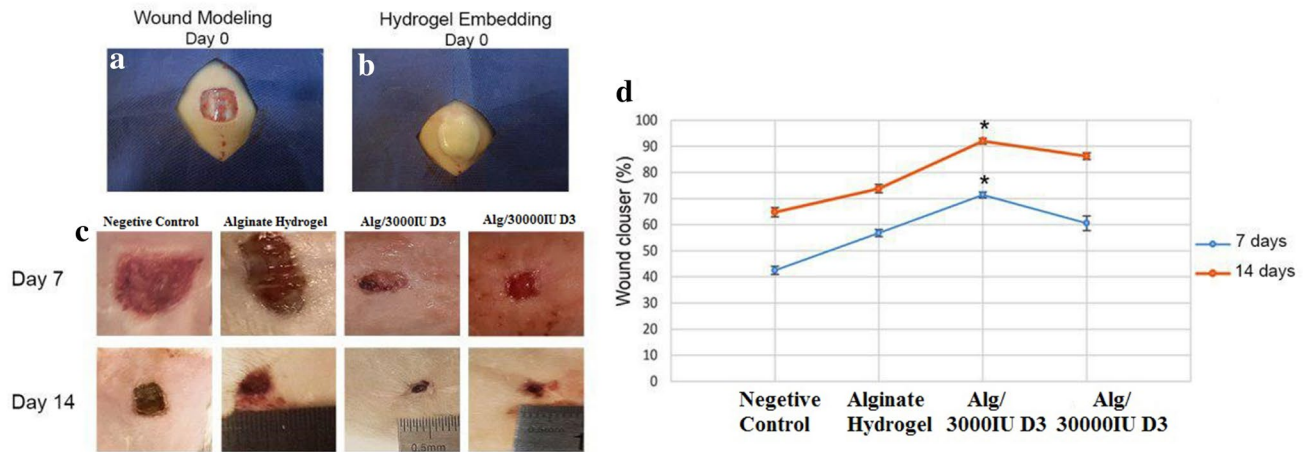


**Fig. 3** **a** Macroscopic image of the wound model created on the dorsum of the rats. **b** Image of wound dressing. **c** Gross morphology of wound healing in the experimental groups at the different time

points. **d** Histogram comparing the wound closure 7th and 14th days post wounding. Asterisk indicates statistically significant difference among the groups ( $p < 0.001$ )

### 3.6 In vivo wound healing study

The healing effects of the prepared hydrogel as the wound dressings were further investigated via the in vivo study and the results are presented in Figs. 3, 4 and 5. As shown in Fig. 3c, there are no signs of infection or inflammation in none of the experimental groups. The microscopic images of the wound healing processes displayed that the wound margin in the Alg/3000 IU D3 sample was unclear and this means the marginal regeneration in the aforementioned group.

The quantitative results of the wound closure percent measurement (Fig. 3d) demonstrated that the Alg/3000 IU D3 group exhibited significantly higher average wound closure than the other groups in both time intervals ( $p < 0.01$ ). The average wound closure for the negative control group on the 7th and 14th days were  $42.5 \pm 0.58\%$  and  $64.8 \pm 1.76\%$ , respectively. However, the highest wound closure percent was observed in the Alg/3000 IU D3 group among all studied groups ( $p < 0.01$ ) with the average wound closure of  $71.42 \pm 0.81\%$  and  $92.03 \pm 1.13\%$  on days 7 and 14 post-wounding, respectively.

### 3.7 Histological and histomorphometric examinations

The wound area monitored over a period of 14 days and histological and histomorphometric examinations were used to qualitatively and quantitatively evaluate the healing effects of the prepared hydrogels. Since the epithelium recovery plays a crucial role in the wound healing process the histological examinations were performed to evaluate the healing degree.

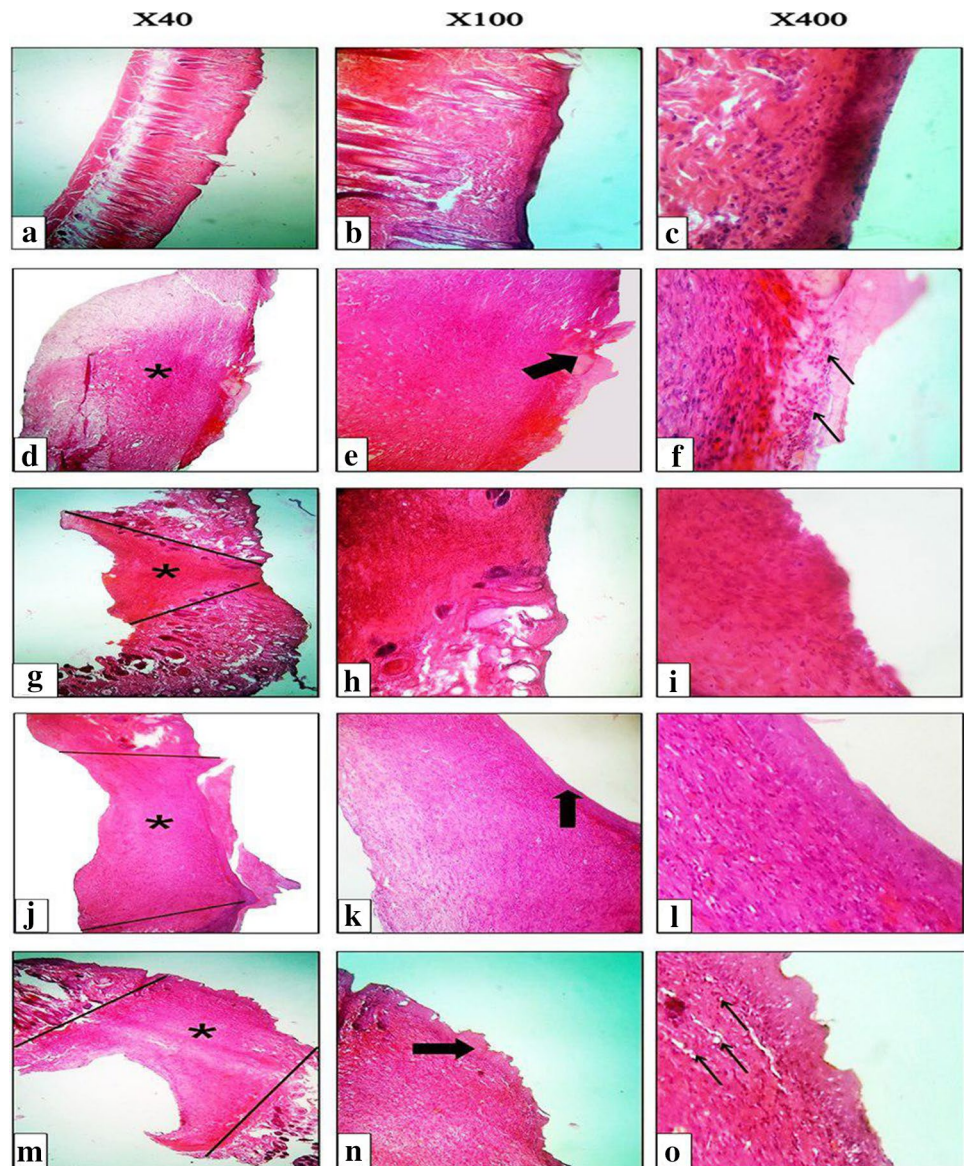
The results showed that the re-epithelialization of Negative Control group ( $0.5 \pm 0.01$ ) was at the minimum degree amongst all groups and the wound was hypocellular with a thin epithelium. On the other hand, the Alg/3000 IU D3 group exhibited the highest re-epithelialization degree ( $4.24 \pm 1.7$ ) and significant healing response compared to the alginate hydrogel ( $0.81 \pm 0.05$ ) and negative control groups ( $p < 0.001$ ). Moreover, Alg/3000 IU D3 group is significantly higher than Alg/30000 IU D3 group ( $2.11 \pm 0.9$ ) ( $p < 0.01$ ).

The alginate hydrogels containing 3000 IU vitamin D<sub>3</sub> had the best performance and induced the highest re-epithelialization and granular tissue formation (Fig. 4k—thick arrow) in the wound site. Histopathology results of Alg/30000 IU D3 group depicted the epidermal proliferation (Fig. 4n—thick arrow), neovascularization (Fig. 4o—thin arrows), and a loose crust of dermal layers in this group. One of the most critical requirements for the skin wound repair is angiogenesis. Interestingly, the histological results revealed that the capillaries formation index of the Alg/3000 IU D3 group was higher than those for the Alginate hydrogel, and Alg/30000 IU D3.

The Masson's trichrome (MT) staining was used to evaluate the collagen formation and deposition during the wound healing process (Fig. 5). The results showed that a low dose of the vitamin D<sub>3</sub> treated group had the greatest collagen thickness (as an important factor for the skin reconstruction). Conversely, the collagen thickness was decreased by increasing the dose of vitamin D<sub>3</sub>/30000 IU. Likewise, the alginate hydrogel group exhibited loose reticular arrangement of collagen.

Based on the histopathological results, it is found that the wound healing degree of the Alg/3000 IU D3 treated group was similar to that of the positive control group (the normal

**Fig. 4** H&E stained microscopic sections of healed incisions in rats at 14 days. **a, b, c** Positive control **d, e, f** Sterile gauze-treated wound, **g, h, i** alginate hydrogel without vitamin D3, **j, k, l** alginate hydrogel/3000 IU vitamin D3, (**m, n, o**) alginate hydrogel/30,000 IU vitamin D3



skin structure without injury, Figs. 4 and 5a–c) at day 14. Among the experimental groups, the best cosmetic appearance was observed in the Alg/3000 IU D3 group in which the neovascularization (Fig. 5l—thin arrows) and growth of hair follicles easily can be seen (Fig. 5k—thick arrows).

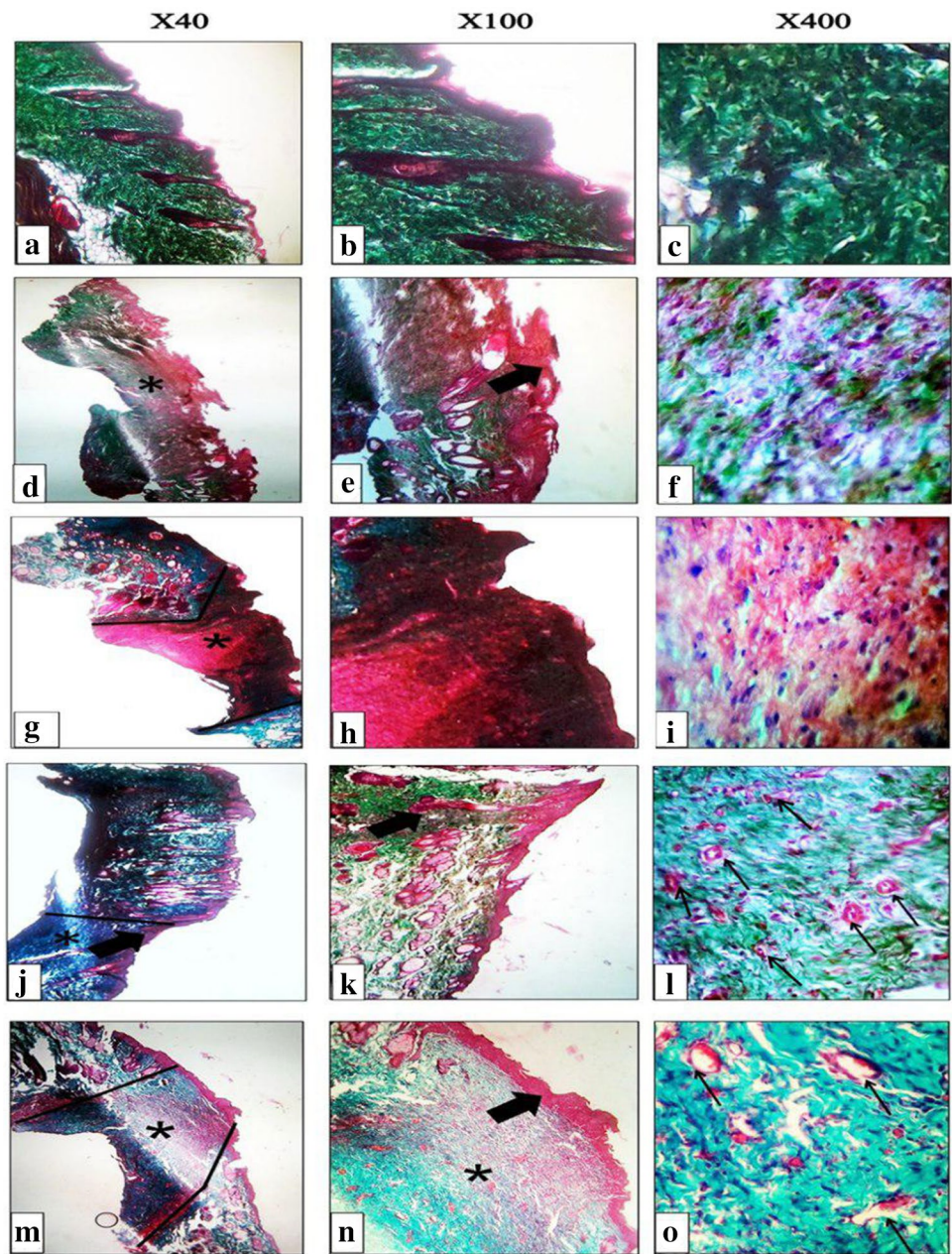
#### 4 Discussion

Recently, many researchers and companies have focused on fabrication and development of the effective wound dressing able to enhance the wound healing process and improve the quality of the regenerated skin. Hydrogel-based biomaterials offer a wide range advantage for skin damage healing due to their interesting properties. The highly porous structure of the hydrogels along with the interconnected pore structure

makes them ideal for tissue regeneration. In a study, Yanas et al. found that the optimal average pore diameter of a proper hydrogel must be neither lower than 20  $\mu\text{m}$  nor higher than 120  $\mu\text{m}$  for skin regeneration purposes [36]. In other words, this pore size range allows the cells to migrate and home inside the pores of the hydrogel-based biomaterials [37]. The analytical results of our study showed that the constructs had a pore size in the range of 75 to 135  $\mu\text{m}$ , which was favorable for cell migration and proliferation [34].

Hydrogels are able to absorb a huge amount of water which make them fascinating drug delivery vehicles. Hydrogels can swell in water and retain a significant deal of water within the 3D cross-linked network without dissolving [38]. In this regard, the interested drug of bioactive molecules can be dissolved in the entrapped water and release from the hydrogel in a controlled manner [39]. Hydrogels can

**Fig. 5** MT stained microscopic sections of healed incisions in rats at 14 days. **a, b, c** Positive control, **d, e, f** Sterile gauze-treated wound, **g, h, i** alginate hydrogel without vitamin D<sub>3</sub>, **j, k, l** alginate hydrogel/3000 IU vitamin D<sub>3</sub>, **m, n, o** alginate hydrogel/30000 IU vitamin D<sub>3</sub>



be exploited as the topical drug delivery for the wounded skin and effectively deliver the healing enhancer agent to the wound. Regarding alginate hydrogel, dry sodium alginate polysaccharide chains interact with water to produce a sol and then, di- or multi-valent cations can cross-link the chains to produce a hydrogel. Cross-linking of surface-attached dry alginate layers by an aqueous CaCO<sub>3</sub> solution resulted in the interconnection of polysaccharide molecules and the formation of a single gel slice (soft hydrogel), which support robust cell growth in vitro [40]. The swelling behavior of ionic hydrogels is affected by the following components; the free energy change of mixing, the free energy changes due to

the network elasticity, and the free energy change resulting from the presence of mobile ions [41].

The degradation rate of hydrogels is another critical parameter which determine the efficacy of the treatment. The degradation rate has a direct correlation with releasing the loaded drug from the matrix of the hydrogel. Our results showed that the degradation rate of the prepared hydrogels is in the acceptable range of 45 to 89%. Moreover, it is observed that the incorporation of vitamin D<sub>3</sub> reduced the degradation rate which can be attributed to the hydrophobic nature of vitamin D<sub>3</sub> [42], which reduces the hydrophilicity of the hydrogel. Besides, it is shown that at higher degrees



of vitamin D<sub>3</sub> (30000 IU), the degradation profile of the scaffold was significantly slower than the other groups.

Hemolysis which is defined as the release of hemoglobin into plasma due to damage of erythrocytes is another important factor for the materials used in skin tissue engineering. Precisely, Wang et al. have shown that hemolysis is directly related to the blood compatibility of materials [43]. We have found that the hemolysis rate of the Alg/30000 IU D3 sample in vitro was lower than the other groups. It was also observed that the addition of vitamin D<sub>3</sub> into the hydrogels decreased the hemolysis rate as compared to hydrogels without this vitamin. This observation can be related to the biocompatibility of vitamin D<sub>3</sub>.

The cell viability and proliferation evaluation conducted with MTT assay showed that the L929 cell seeded on the hydrogels loaded with vitamin D<sub>3</sub> 3000 IU exhibited the highest proliferation rate compared with the other groups at 24 and 72 h post cell culture. Moreover, our results revealed a dose-dependent cell growth indicating the positive effect of the incorporating vitamin D<sub>3</sub> on cell proliferation. These results are in agreement with Bollag WB et al. report which confirmed the positive effect of vitamin D<sub>3</sub> on keratinocyte cell growth [44].

The efficacy of hydrogels containing vitamin D<sub>3</sub> as a wound dressing was also evaluated via the in vivo evaluation. The results showed that the prepared hydrogel-based dressings had the higher wound closure present than the gauze-treated wound (negative control) and the highest wound closure percentage was obtained with the Alg/3000 IU D3 group. This observation is related to the proliferative effect of vitamin D<sub>3</sub> on keratinocyte and fibroblast cells [24, 45].

Oxidative stress induced by reactive oxygen species (ROS) has the inhibitory effect on the wound healing due to the harmful effects on healthy tissues and cells functions [46]. Antioxidant materials and biomolecules can eliminate these harmful effects and improve the healing process [47]. Vitamin D3 is a well-known biological agent that can act as an anti-inflammatory and anti-oxidant factor through various mechanisms such as inducing the several molecules expression involved in the antioxidant active defense system including GSH, GSH peroxidase, and SOD [48]. The observed positive effects of vitamin D<sub>3</sub> on healing efficacy in vivo can be related to the antioxidant activity of vitamin D<sub>3</sub>.

Neovascularization plays a vital role in the skin wound healing process which mediates oxygen and metabolites delivery to the tissues and subsequently maintains the newly formed granulation tissue and the survival of keratinocytes [49]. The histopathological evaluation revealed that the alginate/vitamin D<sub>3</sub> treated wounds also increases angiogenesis in vivo. This effect on angiogenesis may be due to the activation of the CD45, CD117, Sca-1 and Flk-1 positive angiogenic myeloid cells (AMC) through the incorporation

of vitamin D<sub>3</sub> [24, 49]. Furthermore, the results of the histomorphometric analysis showed that Alg/3000 IU D3 represent the highest angiogenesis and re-epithelialization indexes [45].

## 5 Conclusion

The main aim of the present study was to evaluate the combined positive effect of alginate hydrogel with vitamin D<sub>3</sub> on the wound healing process. We fabricated sodium alginate hydrogel containing vitamin D<sub>3</sub> and after characterization, their wound healing efficacy was assessed in the animal model. Our results showed that the properties of the alginate hydrogels are favorable for the skin wound dressing applications. In vitro cell growth study confirmed that the Alg/3000 IU D3 properly induced cells proliferation and the highest cell growth was observed in this group. Furthermore, the in vitro evaluation results indicated that the Alg/3000 IU D3 was capable to accelerate wound healing. Neo-tissue and granulation tissue formation significantly were seen in Alg/3000 IU D3 group compared to other groups. The findings of this experiment suggest that the prepared dressing based on alginate/vitamin D<sub>3</sub> hydrogels are promising for successful skin wound treatment.

**Acknowledgements** The authors gratefully acknowledge the research council of Kermanshah University of Medical Sciences (Grant No. 980769) for financial support.

**Funding** Not applicable.

## Compliance with ethical standards

**Conflict of interest** The authors declare that they have no competing interests.

**Ethical approval** All applicable international, national, and/or institutional guidelines for the care and use of animals were followed.

## References

1. Zhong S, Zhang Y, Lim C. Tissue scaffolds for skin wound healing and dermal reconstruction. *Wiley interdisciplinary reviews. Nanomed Nanobiotechnol.* 2010;2(5):510–25.
2. Allgöwer M, Schoenenberger G, Sparkes B. Burning the largest immune organ. *Burns.* 1995;21:S7–47.
3. Balasubramani M, Kumar TR, Babu M. Skin substitutes: a review. *Burns.* 2001;27(5):534–44.
4. Valizadeh A, Bakhtiary M, Akbarzadeh A, Salehi R, Frakhani SM, Ebrahimi O, Rahmati-yamchi M, Davaran S. Preparation and characterization of novel electrospun poly ( $\epsilon$ -caprolactone)-based nanofibrous scaffolds. *Artif Cells Nanomed Biotechnol.* 2016;44(2):504–9.

5. Mir M, Ali MN, Barakullah A, Gulzar A, Arshad M, Fatima S, Asad M. Synthetic polymeric biomaterials for wound healing: a review. *Progr Biomater*. 2018;7(1):1–21.
6. Kamoun EA, Kenawy E-RS, Chen X. A review on polymeric hydrogel membranes for wound dressing applications: pVA-based hydrogel dressings. *J Adv Res*. 2017;8(3):217–33.
7. Varaprasad K, Jayaramudu T, Kanikireddy V, Toro C, Sadiku ER. Alginate-based composite materials for wound dressing application: a mini review. *Carbohydr Polym*. 2020. <https://doi.org/10.1016/j.carbpol.2020.116025>.
8. El-Sherbiny IM, Yacoub MH. Hydrogel scaffolds for tissue engineering: progress and challenges. *Glob Cardiol Sci Pract*. 2013. <https://doi.org/10.5339/gcsp.2013.38>.
9. Abbasian M, Massoumi B, Mohammad-Rezaei R, Samadian H, Jaymand M. Scaffolding polymeric biomaterials: are naturally occurring biological macromolecules more appropriate for tissue engineering? *Int J Biol Macromol*. 2019;134:673–94. <https://doi.org/10.1016/j.ijbiomac.2019.04.197>.
10. Massoumi B, Mozaffari Z, Jaymand M. A starch-based stimuli-responsive magnetite nanohydrogel as de novo drug delivery system. *Int J Biol Macromol*. 2018;117:418–26.
11. Mozaffari Z, Hatamzadeh M, Massoumi B, Jaymand M. Synthesis and characterization of a novel stimuli-responsive magnetite nanohydrogel based on poly (ethylene glycol) and poly (N-isopropylacrylamide) as drug carrier. *J Appl Polym Sci*. 2018;135(36):46657.
12. Hoare TR, Kohane DS. Hydrogels in drug delivery: progress and challenges. *Polymer*. 2008;49(8):1993–2007.
13. Abbasian M, Bakhshi M, Jaymand M, Karaj-Abad SG. Nitroxide-mediated graft copolymerization of styrene from cellulose and its polymer/montmorillonite nanocomposite. *J Elastomers Plast*. 2019;51(5):473–89.
14. Sun J, Tan H. Alginate-based biomaterials for regenerative medicine applications. *Materials*. 2013;6(4):1285–309.
15. Ma PX. Scaffolds for tissue fabrication. *Mater Today*. 2004;7(5):30–40. [https://doi.org/10.1016/S1369-7021\(04\)00233-0](https://doi.org/10.1016/S1369-7021(04)00233-0).
16. Pereira R, Carvalho A, Vaz DC, Gil M, Mendes A, Bártolo P. Development of novel alginate based hydrogel films for wound healing applications. *Int J Biol Macromol*. 2013;52:221–30.
17. Murakami K, Aoki H, Nakamura S, Nakamura S-i, Takikawa M, Hanzawa M, Kishimoto S, Hattori H, Tanaka Y, Kiyosawa T. Hydrogel blends of chitin/chitosan, fucoidan and alginate as healing-impaired wound dressings. *Biomaterials*. 2010;31(1):83–90.
18. Balakrishnan B, Mohanty M, Umashankar P, Jayakrishnan A. Evaluation of an in situ forming hydrogel wound dressing based on oxidized alginate and gelatin. *Biomaterials*. 2005;26(32):6335–42.
19. Suganya S, Venugopal J, Mary SA, Ramakrishna S, Lakshmi B, Dev VG. Aloe vera incorporated biomimetic nanofibrous scaffold: a regenerative approach for skin tissue engineering. *Iran Polym J*. 2014;23(3):237–48.
20. Ninan N, Muthiah M, Park I-K, Wong TW, Thomas S, Grohens Y. Natural polymer/inorganic material based hybrid scaffolds for skin wound healing. *Polym Rev*. 2015;55(3):453–90.
21. Dzikowski M, Castanié N, Guedon A, Verrier B, Primard C, Sohier J. Antibiotic incorporation in jet-sprayed nanofibrillar biodegradable scaffolds for wound healing. *Int J Pharm*. 2017;532(2):802–12.
22. Tian XQ, Chen TC, Holick MF. 1, 25-Dihydroxyvitamin D<sub>3</sub>: a novel agent for enhancing wound healing. *J Cell Biochem*. 1995;59(1):53–6.
23. Smith EL, Walworth NC, Holick MF. Effect of 1 $\alpha$ , 25-dihydroxyvitamin D<sub>3</sub> on the morphologic and biochemical differentiation of cultured human epidermal keratinocytes grown in serum-free conditions. *J Invest Dermatol*. 1986;86(6):709–14.
24. Wong MSK, Leisegang MS, Kruse C, Vogel J, Schürmann C, Dehne N, Weigert A, Herrmann E, Brüne B, Shah AM. Vitamin D promotes vascular regeneration. *Circulation*. 2014;114:010650.
25. Sadat-Ali M, Bubshait DA, Al-Turki HA, Al-Dakheel DA, Al-Olayani WS. Topical delivery of vitamin D<sub>3</sub>: a randomized controlled pilot study. *Int J Biomed Sci IJBS*. 2014;10(1):21.
26. Ramezani T, Kilfoyle BE, Zhang Z, Michniak-Kohn BB. Polymeric nanospheres for topical delivery of vitamin D<sub>3</sub>. *Int J Pharm*. 2017;516(1–2):196–203.
27. Lehmann B. Role of the vitamin D<sub>3</sub> pathway in healthy and diseased skin—facts, contradictions and hypotheses. *Exp Dermatol*. 2009;18(2):97–108.
28. Jang J, Seol Y-J, Kim HJ, Kundu J, Kim SW, Cho D-W. Effects of alginate hydrogel cross-linking density on mechanical and biological behaviors for tissue engineering. *J Mech Behav Biomed Mater*. 2014;37:69–77.
29. Bagher Z, Ehterami A, Safdel MH, Khastar H, Semiari H, Asefnjad A, Davachi SM, Mirzaii M, Salehi M. Wound healing with alginate/chitosan hydrogel containing hesperidin in rat model. *J Drug Deliv Sci Technol*. 2020;55:101379.
30. Samadian H, Vaez A, Ehterami A, Salehi M, Farzamfar S, Sahrapeyma H, Norouzi P. Sciatic nerve regeneration by using collagen type I hydrogel containing naringin. *J Mater Sci Mater Med*. 2019;30(9):107.
31. Ghorbani S, Tiraihi T, Soleimani M. Differentiation of mesenchymal stem cells into neuron-like cells using composite 3D scaffold combined with valproic acid induction. *J Biomater Appl*. 2018;32(6):702–15.
32. Alizadeh R, Bagher Z, Kamrava SK, Falah M, Hamidabadi HG, Boroujeni ME, Mohammadi F, Khodaverdi S, Zare-Sadeghi A, Olya A. Differentiation of human mesenchymal stem cells (MSC) to dopaminergic neurons: a comparison between Wharton's Jelly and olfactory mucosa as sources of MSCs. *J Chem Neuroanat*. 2019;96:126–33.
33. Salehi M, Vaez A, Naseri-Nosar M, Farzamfar S, Ai A, Ai J, Tavakol S, Khakbiz M, Ebrahimi-Barough S. Naringin-loaded poly( $\epsilon$ -caprolactone)/gelatin electrospun mat as a potential wound dressing: in vitro and in vivo evaluation. *Fibers Polym*. 2018;19(1):125–34.
34. Yang S, Leong K-F, Du Z, Chua C-K. The design of scaffolds for use in tissue engineering. Part I. Traditional factors. *Tissue Eng*. 2001;7(6):679–89.
35. Zusiak SP, Leach JB. Hydrolytically degradable poly(ethylene glycol) hydrogel scaffolds with tunable degradation and mechanical properties. *Biomacromol*. 2010;11(5):1348–57.
36. Yannas I, Lee E, Orgill DP, Skrabut E, Murphy GF. Synthesis and characterization of a model extracellular matrix that induces partial regeneration of adult mammalian skin. *Proc Natl Acad Sci*. 1989;86(3):933–7.
37. O'Brien FJ, Harley B, Yannas IV, Gibson LJ. The effect of pore size on cell adhesion in collagen-GAG scaffolds. *Biomaterials*. 2005;26(4):433–41.
38. Shi J, Xing MM, Zhong W. Development of hydrogels and biomimetic regulators as tissue engineering scaffolds. *Membranes*. 2012;2(1):70–90.
39. Kuo CK, Ma PX. Ionically crosslinked alginate hydrogels as scaffolds for tissue engineering: part 1. Structure, gelation rate and mechanical properties. *Biomaterials*. 2001;22(6):511–21.
40. Matyash M, Despang F, Ikonomidou C, Gelinsky M. Swelling and mechanical properties of alginate hydrogels with respect to promotion of neural growth. *Tissue Eng Part C Methods*. 2013;20(5):401–11.
41. Takeno H, Kimura Y, Nakamura W. Mechanical, swelling, and structural properties of mechanically tough clay-sodium polyacrylate blend hydrogels. *Gels*. 2017;3(1):10.

42. Romagnoli E, Pepe J, Piemonte S, Cipriani C, Minisola S. Management of endocrine disease: value and limitations of assessing vitamin D nutritional status and advised levels of vitamin D supplementation. *Eur J Endocrinol.* 2013;169(4):R59–69.
43. Wang M, Yuan J, Huang X, Cai X, Li L, Shen J. Grafting of carboxybetaine brush onto cellulose membranes via surface-initiated ARGET-ATRP for improving blood compatibility. *Colloids Surf B.* 2013;103:52–8.
44. Bollag WB, Ducote J, Harmon CS. Biphasic effect of 1, 25-dihydroxyvitamin D3 on primary mouse epidermal keratinocyte proliferation. *J Cell Physiol.* 1995;163(2):248–56.
45. Rougui Z, Pavlovitch J, Rizk-Rabin M. In vivo effects of vitamin D on the proliferation and differentiation of rat keratinocytes. *J Cell Physiol.* 1996;168(2):385–94.
46. Aliyev E, Sakallıoğlu U, Eren Z, Açıkgöz G. The effect of polylactide membranes on the levels of reactive oxygen species in periodontal flaps during wound healing. *Biomaterials.* 2004;25(19):4633–7.
47. Farzamfar S, Naseri-Nosar M, Samadian H, Mahakizadeh S, Tajerian R, Rahmati M, Vaez A, Salehi M. Taurine-loaded poly ( $\epsilon$ -caprolactone)/gelatin electrospun mat as a potential wound dressing material: In vitro and in vivo evaluation. *J Bioact Compat Polym.* 2017;33(3):282–94. <https://doi.org/10.1177/0883911517737103>.
48. Mokhtari Z, Hekmatdoost A, Nourian M. Antioxidant efficacy of vitamin D. *J Parathyr Dis.* 2017;5(1):12.
49. Wu Y, Chen L, Scott PG, Tredget EE. Mesenchymal stem cells enhance wound healing through differentiation and angiogenesis. *Stem Cells.* 2007;25(10):2648–59.

**Publisher's Note** Springer Nature remains neutral with regard to jurisdictional claims in published maps and institutional affiliations.